Embodied Intelligence in Soft Robots: Strides in Morphological Computation for Control

Lekan Molu

Microsoft Research

New York City, NY 10012

Presented by **Lekan Molu** (Lay-con Mo-lu)

October 31, 2024

Talk Overview

- The principle of morphological computation in nature
  - Morphology: shape, geometry, and mechanical properties.
  - Computation: sensorimotor information transmission among geometrical components.
- Morphology and computation in artificial robots
  - Cosserat Continua and reduced soft robot models.
  - **Reductions**: Structural Lagrangian properties and control.
- Towards real-time strain regulation and control
  - **Simplexity**: Hierarchical and fast versatile control with reduced variables.

Morphology and computation

- Morphology: Emergent behaviors of natural organisms from complex sensorimotor nonlinear mechanical feedback from the environment.
  - Shape affecting behavioral response.
  - Geometrical Arrangement of motors such that processing and perception affect computational characteristics.
  - Mechanical properties that allow the engineering of emergent behaviors via adaptive environmental interaction.
- Computation: The information transformation among the system geometrical units, upon environmental perception, that effect morphological changes in shape and material properties.

MC in vertebrates – a case for soft designs

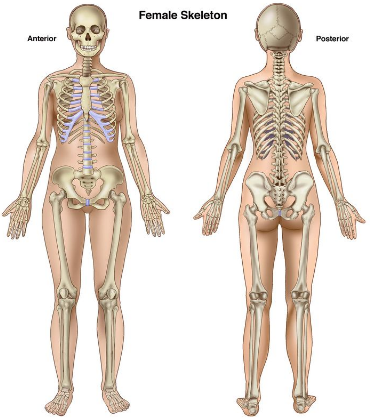

An adult human skeleton $\approxeq 11\%$ of the body mass. ©Brittanica

- The arrangement and compliance of body parts, perception, and computation creates emergence of complex interactive behavior.
- Soft bodies seem critical to the emergence of adaptive natural behaviors.
- Morphological computation is crucial in the design of robots that execute adaptive natural behavior.

MC in Vertebrates: The Central Pattern Generator

- A neural mechanism (in vertebrates) that generates motor control with minimal parameters.
- CPG: Neurons and synapses couple to generate effective motor activation for rhythmic environmental motion.
  - In Lampreys, only two signals trigger swimming motion, for example!
  - This CPG enables indirect use of brain computational power via nonlinear feedback from stretch receptor neurons on Lamprey's skin.

Simplexity in Morphological Computation

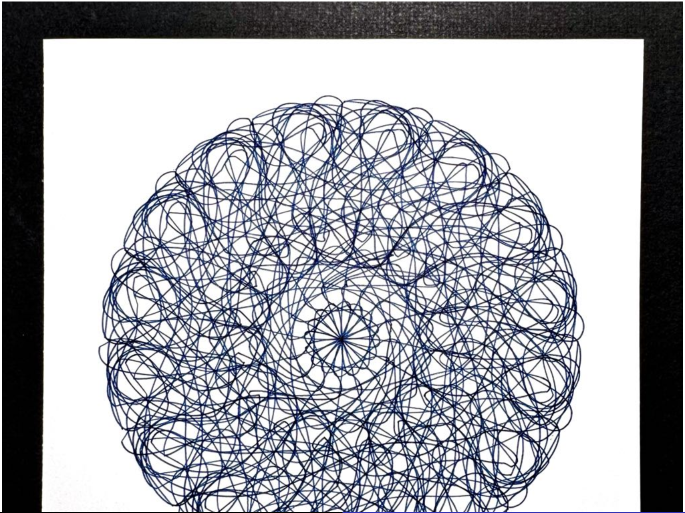

Simplexity in Morphological Computation

- Simplexity: Exploiting structure for effective control.
  - The geometrical tuning of the morphology and neural circuitry in the brain of mammals that simplify the perception and control of complex natural phenomena.
  - Not exactly simplified models or reduced complexity.
  - But rather, sparse connections and finite variables to execute adaptive sensorimotor strategies!
- Example: Saccades (focused eye movements) are controlled by (small) Superior Colliculus in the human brain.
  - Plug: Complex neural circuitry; simple control systems!

Morphing in Invertebrates: Cephalopods

Cuttlefish. ©Monterey Bay Museum

Octopus. ©Smithsonian Magazine

The Octopus and Cuttlefish

- No exoskeleton, or spinal cord.
- A muscular hydrostat: transversal, longitudinal, and oblique muscles along richly innervated arms and mechanoreceptors:
  - Allows for bending, stretching, stiffening, and retraction.
  - Diverse compliance across eight arms imply sophisticated motion strategies in the wild!
- Simplexity enhanced by a peripheral nervous system and a central nervous system.

Soft Robot Mechanism in Focus

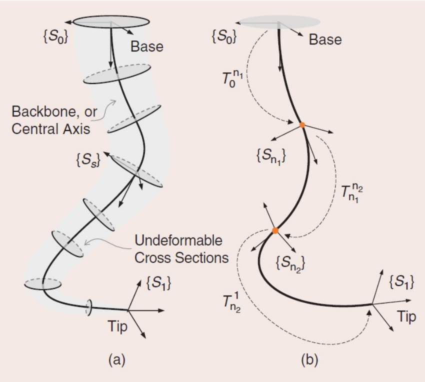

A continuum soft robot whose mechanics can be well-described with Cosserat rod theory. Reprinted from (Della Santina et al. (2023))

- One dimension is quintessentially longer than the other two.
- Characterized by a central axis with undeformable discs that characterize deformable cross-sectional segments.
- Strain and deformation, via e.g. Cosserat rod theory, enables precise finite-dimensional mathematical models.

A Finite and Reliable Model

- A soft robot's usefulness is informed by control system that melds its body deformation with internal actuators.
- By design, this calls for a high-fidelity model or a delicate balancing of complex morphology and data-driven methods.

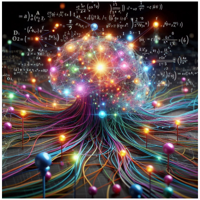

- Non-interpretable; non-reliable.
- $\times$Continuous coupled interaction between the material, actuators, and external affordances.

The case for model-based control

- Soft robots are infinite degrees-of-freedom continua i.e., PDEs are the main tools for analysis.
- nonlinear PDE theory is tedious and computationally intensive.
- Notable strides in reduced-order, finite-dimensional mathematical models that induce tractability in continuum models.

Tractable reduced-order models

- Morphoelastic filament theory: Moulton et al. (2020); Kaczmarski et al. (2023); Gazzola et al. (2018);
- Generalized Cosserat rod theory: Rubin (2000); Cosserat and Cosserat (1909);
- The constant curvature model: Godage et al. (2011);
- The piecewise constant curvature model: Webster and Jones (2010); Qiu et al. (2023); and
- Ordinary differential equations-based discrete Cosserat model: Renda et al. (2016, 2018).

Model-based control

- The discrete Cosserat model Renda et al. (2018).
  - Restricting possible emergent shapes to a finite-dimensional functional space
  - Space is a curve, $X : [0, L]$, that parameterizes the robot.
  - Essentially take finite nodal points on robot's body $\rightarrow$ approximate dynamics along the discrete sections by an ordinary differential equations (ODE).
- Control can be realized to arbitrary precision, constrained by discretization space.

Modeling Analysis – Basic Taxonomy

- Strain-parameterized dynamics on a reduced special Euclidean-3 group (SE(3)).
- C-space: $g(X) : X \rightarrow \mathbb{SE}(3) = \begin{pmatrix} \boldsymbol{R}(X) & \boldsymbol{p}(X) \\ 0^\top & 1 \end{pmatrix}$.
- Strain and twist vectors: $\{\boldsymbol{\eta}, \xi\} \in \mathbb{R}^6$.
- Strain field: $\breve{\boldsymbol{\eta}}(X) = g^{-1}\partial g/\partial X$.
- Twist field: $\breve{\xi}(X) = g^{-1}\partial g/\partial t$.

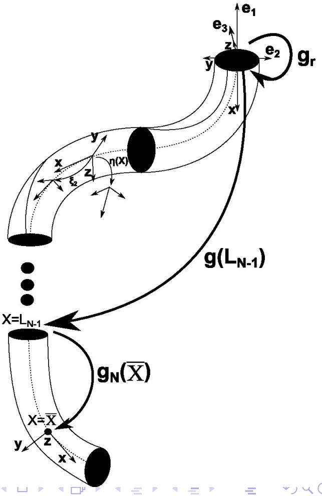

The Discrete Cosserat Model

- $X \in [0, L]$ is divided into N intervals: $[0, L_1], \cdots, [L_{N-1}, L_N]$.
- In Renda et al. (2018)'s proposition, the robot's mass divides into N discrete sections $\{\mathcal{M}_n\}_{n=1}^{N}$;
- Each with constant strain $\boldsymbol{\eta}_n$
- Strain field: $\breve{\boldsymbol{\eta}}(X) = g^{-1}\partial g/\partial X$.
- Twist field: $\breve{\xi}(X) = g^{-1}\partial g/\partial t$.

Dynamic Equations of the Rod-like Arm

$$\underbrace{\left[\int_0^{L_N} J^T \mathcal{M}_a J dX\right]}_{M(q)} \ddot{q} + \underbrace{\left[\int_0^{L_N} J^T \mathrm{ad}^\star_{J\dot{q}} \mathcal{M}_a J dX\right]}_{C_1(q,\dot{q})} \dot{q} +$$

$$\underbrace{\left[\int_0^{L_N} J^T \mathcal{M}_a \dot{J} dX\right]}_{C_2(q,\dot{q})} \dot{q} + \underbrace{\left[\int_0^{L_N} J^T \mathcal{D} J \|J\dot{q}\|_p dX\right]}_{D(q,\dot{q})} \dot{q}$$

$$- \underbrace{(1 - \rho_f/\rho)\left[\int_0^{L_N} J^T \mathcal{M} \mathrm{Ad}_{\boldsymbol{g}}^{-1} dX\right]}_{N(q)} \mathrm{Ad}_{\boldsymbol{g}_r}^{-1} \mathcal{G} - \underbrace{J(\bar{X})^T \mathcal{F}_p}_{F(q)}$$

$$- \int_0^{L_N} J^T \left[\nabla_x \mathcal{F}_i - \nabla_x \mathcal{F}_a + \mathrm{ad}^\star_{\xi_n}(\mathcal{F}_i - \mathcal{F}_a)\right] dX = 0, \quad (1)$$

Structural Properties of Rod-like Robots

$$M(\boldsymbol{q})\ddot{\boldsymbol{q}} + \left[C_1(q, \dot{\boldsymbol{q}}) + C_2(\boldsymbol{q}, \dot{\boldsymbol{q}})\right] \dot{\boldsymbol{q}} = F(\boldsymbol{q}) + N(\boldsymbol{q})\text{Ad}_{\boldsymbol{g}_r}^{-1}\mathcal{G} + \tau(\boldsymbol{q}) - D(\boldsymbol{q}, \dot{\boldsymbol{q}})\dot{\boldsymbol{q}}. \tag{2}$$

Property 1 (Positive definiteness of the Inertia Operator)

The inertia tensor $\mathcal{M}_a(\boldsymbol{q})$ is symmetric and positive definite. As a result $M(\boldsymbol{q})$ is symmetric and positive definite.

Proof.

The jacobian, J, is injective by (Renda et al., 2018, equation 20). Thus, property 1 follows from its definition. □

Structural Properties of Rod-like Robots

Property 2 (Boundedness of the Mass Matrix)

The mass inertial matrix $M(\boldsymbol{q})$ is uniformly bounded from below by $m\boldsymbol{I}$ where m is a positive constant and $\boldsymbol{I}$ is the identity matrix.

Proof of Property 2.

This is a restatement of the lower boundedness of $M(\boldsymbol{q})$ for fully actuated n-degrees of freedom manipulators Romero et al. (2014). □

Structural Properties of Rod-like Robots

Property 3 (Skew symmetric property)

The matrix $\dot{M}(\boldsymbol{q}) - 2\left[C_1(\boldsymbol{q}, \dot{\boldsymbol{q}}) + C_2(\boldsymbol{q}, \dot{\boldsymbol{q}})\right]$ *is skew-symmetric.*

Proof of Property 3.

TL; DR: See proof in Molu and Chen (2024). □

Skew-Symmetric Property Proof

By Leibniz's rule, we have

$$\dot{M}(\boldsymbol{q}) = \frac{d}{dt}\left(\int_0^{L_N} J^T \mathcal{M}_a J dX\right) = \int_0^{L_N} \frac{\partial}{\partial t}\left(J^T \mathcal{M}_a J\right) dX$$
$$\triangleq \int_0^{L_N} \left(\dot{J}^T \mathcal{M}_a J + J^T \dot{\mathcal{M}}_a J + J^T \mathcal{M}_a \dot{J}\right) dX. \tag{3}$$

Therefore, $\dot{M}(\boldsymbol{q}) - 2\left[C_1(\boldsymbol{q}, \dot{\boldsymbol{q}}) + C_2(\boldsymbol{q}, \dot{\boldsymbol{q}})\right]$ becomes

$$\int_0^{L_N} \left(\dot{J}^\top \mathcal{M}_a J + J^\top \dot{\mathcal{M}}_a J + J^\top \mathcal{M}_a \dot{J}\right) dX - 2\int_0^{L_N} \left(J^\top \text{ad}^\star_{J\dot{\boldsymbol{q}}} \mathcal{M}_a J + J^\top \mathcal{M}_a \dot{J}\right) dX \tag{4}$$

$$\triangleq \int_0^{L_N} \left(\dot{J}^\top \mathcal{M}_a J + J^\top \dot{\mathcal{M}}_a J - J^\top \mathcal{M}_a \dot{J}\right) dX - 2\int_0^{L_N} J^\top \text{ad}^\star_{J\dot{\boldsymbol{q}}} \mathcal{M}_a J dX. \tag{5}$$

Skew-Symmetric Property Proof

Similarly, $-\left[\dot{M}(\boldsymbol{q}) - 2\left[C_1(\boldsymbol{q},\dot{\boldsymbol{q}}) + C_2(\boldsymbol{q},\dot{\boldsymbol{q}})\right]\right]^\top$ expands as

$$
\begin{aligned}
&-\dot{M}^\top(\boldsymbol{q}) + 2\left[C_1^\top(\boldsymbol{q},\dot{\boldsymbol{q}}) + C_2^\top(\boldsymbol{q},\dot{\boldsymbol{q}})\right] = \\
&\int_0^{L_N} dX^\top \left(-J^\top \mathcal{M}_a \dot{J} - J^\top \dot{\mathcal{M}}_a J - \dot{J}^\top \mathcal{M}_a J\right) + 2\int_0^{L_N} dX^\top \left(J^\top \mathcal{M}_a \mathrm{ad}_{J\dot{\boldsymbol{q}}} J + \dot{J}^\top \mathcal{M}_a J\right) \\
&\triangleq \int_0^{L_N} \left(J^\top \mathcal{M}_a \dot{J} - \dot{J}^\top \mathcal{M}_a J - J^\top \dot{\mathcal{M}}_a J\right) dX - 2\int_0^{L_N} J^\top \mathrm{ad}^\star_{J\dot{\boldsymbol{q}}} \mathcal{M}_a J dX \qquad (6)
\end{aligned}
$$

which satisfies the identity:

$$
\begin{aligned}
\dot{M}(\boldsymbol{q}) - 2\left[C_1(\boldsymbol{q},\dot{\boldsymbol{q}}) + C_2(\boldsymbol{q},\dot{\boldsymbol{q}})\right] = \\
-\left[\dot{M}(\boldsymbol{q}) - 2\left[C_1(\boldsymbol{q},\dot{\boldsymbol{q}}) + C_2(\boldsymbol{q},\dot{\boldsymbol{q}})\right]\right]^\top. \qquad (7)
\end{aligned}
$$

A fortiori, the skew symmetric property follows.

MC Takeaways: Simplexity

- Simplexity: Reliance on a few parameters to model an infinite-DoF system:

$$M(q)\ddot{q} + \left[C_1(q,\dot{q}) + C_2(q,\dot{q})\right]\dot{q} = F(q) + N(q)\mathrm{Ad}_{\boldsymbol{g}_r}^{-1}\mathcal{G} + \tau(q) - D(q,\dot{q})\dot{q}.$$

- Simplexity: From PDE to ODE, i.e. inifinite-dimensional analysis (Continuum PDE) to finite-dimensional ODE!
- Computation of deformation is possible at finite nodal points.

Computational Control exploiting structural properties

- Proposal: A globally asymptotically stabilizing proportional-derivative (PD) controller for a rod-like soft arm.
  - Regarding the generalized torque $\tau(\boldsymbol{q})$ as a control input, $u(\boldsymbol{q}, \dot{\boldsymbol{q}})$, feedback laws are sufficient for attaining a desired soft body configuration.

Theorem 1 (Cable-driven Actuation)

For positive definite diagonal matrix gains K_D and K_p, without gravity/buoyancy compensation, the control law

$$u(\boldsymbol{q}, \dot{\boldsymbol{q}}) = -K_p \tilde{\boldsymbol{q}} - K_D \dot{\boldsymbol{q}} - F(\boldsymbol{q}) \tag{8}$$

under a cable-driven actuation globally asymptotically stabilizes system (2), where $\tilde{\boldsymbol{q}}(t) = \boldsymbol{q}(t) - \boldsymbol{q}^d$ is the joint error vector for a desired equilibrium point $\boldsymbol{q}^d$.

Computational Control exploiting structural properties

Corollary 2 (Fluid-driven actuation)

If the robot is operated without cables, and is driven with a dense medium such as pressurized air or water, then the term $F(\boldsymbol{q}) = 0$ *so that the control law* $u(\boldsymbol{q}, \dot{\boldsymbol{q}}) = -K_p\tilde{\boldsymbol{q}} - K_D\dot{\boldsymbol{q}}$ *globally asymptotically stabilizes the system.*

Proof.

Proofs in Section V of Molu and Chen (2024). □

Computational Control exploiting structural properties

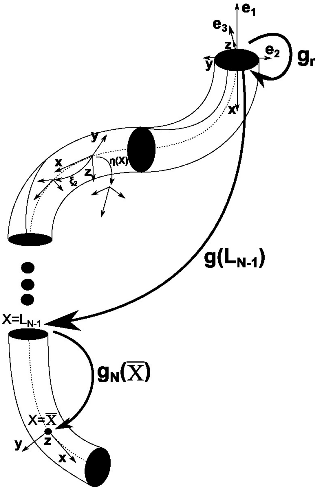

- Tip load in the $+y$ direction in the robot's base frame.
- Poisson ratio: 0.45; $\mathcal{M} = \rho[I_x, I_y, I_z, A, A, A]$ with $\rho = 2,000kgm^{-3}$ following Renda et al. (2018).
- $A = \pi r^2$; $D = -\rho_w \nu^T \nu \check{D} \nu / |\nu|$.
- $X \in [0, L]$ discretized into 41 segments for each experiment.

Computational Control exploiting structural properties

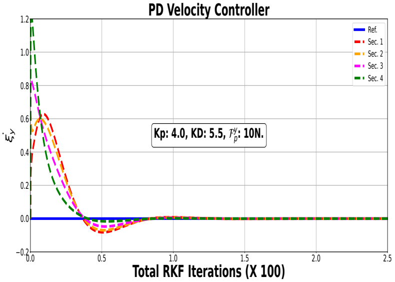

Cable-driven, strain twist setpoint terrestrial control.

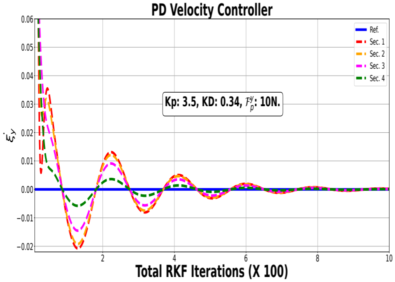

Fluid-actuated, strain twist setpoint terrestrial control.

Computational Control exploiting structural properties

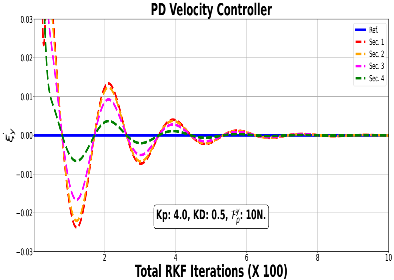

Fluid-actuated, strain twist setpoint underwater control.

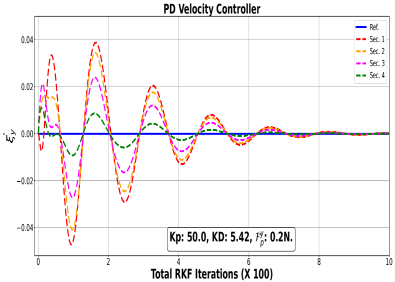

Cable-driven, strain twist setpoint regulation.

Computational Control exploiting structural properties

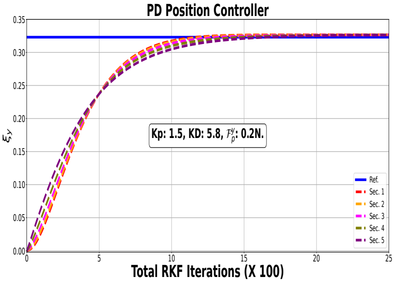

Cable-based position control with a small tip load, 0.2N.

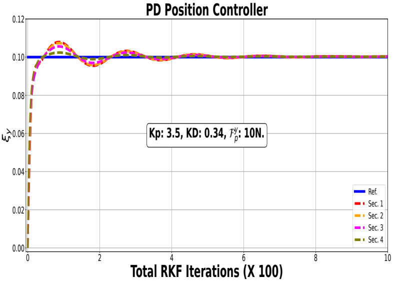

Terrestrial position control.

Exploiting Mechanical Nonlinearity for Feedback!

This page is left blank intentionally.

Hierarchical Dynamics and Control

- Reaching steps towards the real-time strain control of multiphysics, multiscale continuum soft robots.
- Separate subdynamics — aided by a perturbing time-scale separation parameter.
- Respective stabilizing nonlinear backstepping controllers.
- Stability of the interconnected singularly perturbed. system.
- Fast numerical results on a single arm of the Octopus robot arm.

Layered control architecture

- Essentially a layered multirate control scheme (Matni et al. (2024)) of the various interconnected physics components of a soft robot prototype.

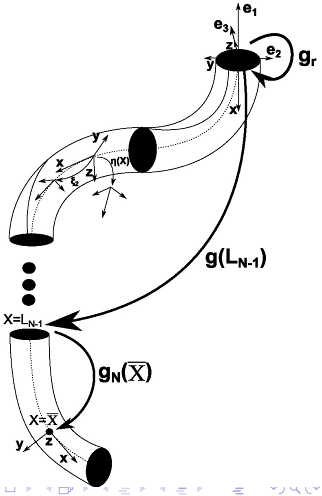

Framework: Singularly Perturbed Dynamics

- A standard two-time-scale singularly perturbed system:

$$\dot{\boldsymbol{z}}_1 = \boldsymbol{f}(\boldsymbol{z}_1, \boldsymbol{z}_2, \epsilon, \boldsymbol{u}_s, t), \;\; \boldsymbol{z}_1(t_0) = \boldsymbol{z}_1(0), \;\; \boldsymbol{z}_1 \in \mathbb{R}^{6N}, \tag{9a}$$

$$\epsilon\dot{\boldsymbol{z}}_2 = \boldsymbol{g}(\boldsymbol{z}_1, \boldsymbol{z}_2, \epsilon, \boldsymbol{u}_f, t), \;\; \boldsymbol{z}_2(t_0) = \boldsymbol{z}_2(0), \;\; \boldsymbol{z}_2 \in \mathbb{R}^{6N} \tag{9b}$$

- $\boldsymbol{f}$ and $\boldsymbol{g}$ are $\mathcal{C}^n(n \gg 0)$ differentiable functions of their arguments;
- $\epsilon > 0$ denotes all small parameters to be ignored.
- $\boldsymbol{u}_s$ is the slow sub-dynamics' control law, and
- $\boldsymbol{u}_f$ is the fast sub-dynamics' controller.

Framework: Slow Dynamics Extraction

Assumption 1 (Real and distinct root)

Equation (9) has the unique and distinct root $\boldsymbol{z}_2 = \phi(\boldsymbol{z}_1, t)$ *(for a sufficiently smooth* ϕ*) so that*

$$0 = \boldsymbol{g}(\boldsymbol{z}_1, \phi(\boldsymbol{z}_1, t), 0, 0, t) \triangleq \bar{\boldsymbol{g}}(\boldsymbol{z}_1, 0, t), \;\; \boldsymbol{z}_1(t_0) = \boldsymbol{z}_1(0). \tag{10}$$

The slow subsystem therefore becomes

$$\dot{\boldsymbol{z}}_1 = \boldsymbol{f}(\boldsymbol{z}_1, \phi(\boldsymbol{z}_1, t), 0, \boldsymbol{u}_s, t) \triangleq \boldsymbol{f}_s(\boldsymbol{z}_1, \boldsymbol{u}_s, t). \tag{11}$$

Framework: Slow Dynamics Extraction

- Assumption: the fast feedback law is asymptotically stable;
  - It does not modify the open-loop equilibrium manifold of the fast dynamics.
- With $\epsilon = 0$ we have,

$$\dot{\boldsymbol{z}}_1 = \boldsymbol{f}(\boldsymbol{z}_1, \boldsymbol{z}_2, 0, \boldsymbol{u}_s, t), \;\; \boldsymbol{z}_1(t_0) = \boldsymbol{z}_1(0), \tag{12a}$$

$$0 = \boldsymbol{g}(\boldsymbol{z}_1, \boldsymbol{z}_2, 0, 0, t). \tag{12b}$$

Framework: Fast Dynamics Extraction

Introduce the time scale $T = t/\epsilon$, and write the deviation of $\boldsymbol{z}_2$ from its isolated equilibrium manifold, $\phi(\boldsymbol{z}_1, t)$ as $\tilde{\boldsymbol{z}}_2 = \boldsymbol{z}_2 - \phi(\boldsymbol{z}_1, t)$. Then, (9) becomes

$$\frac{d\boldsymbol{z}_1}{dT} = \epsilon \boldsymbol{f}(\boldsymbol{z}_1, \tilde{\boldsymbol{z}}_2 + \phi(\boldsymbol{z}_1, t), \epsilon, \boldsymbol{u}_s, t), \tag{13a}$$

$$\frac{d\tilde{\boldsymbol{z}}_2}{dT} = \epsilon \frac{d\boldsymbol{z}_2}{dt} - \epsilon \frac{\partial \phi}{\partial \boldsymbol{z}_1} \dot{\boldsymbol{z}}_1, \tag{13b}$$

$$= \boldsymbol{g}(\boldsymbol{z}_1, \tilde{\boldsymbol{z}}_2 + \phi(\boldsymbol{z}_1, t), \epsilon, \boldsymbol{u}_f, t) - \epsilon \frac{\partial \phi(\boldsymbol{z}_1, t)}{\partial \boldsymbol{z}_1} \dot{\boldsymbol{z}}_1. \tag{13c}$$

Framework for singularly perturbed dynamics

Setting $\epsilon = 0$, we obtain the algebraic equation

$$\frac{d\tilde{\boldsymbol{z}}_2}{dT} = \boldsymbol{g}(\boldsymbol{z}_1, \tilde{\boldsymbol{z}}_2 + \phi(z_1, t), 0, \boldsymbol{u}_f, t) \tag{14}$$

with $\boldsymbol{z}_1$ frozen to its initial values.

Decomposition of SoRo Rod Dynamics

This page is left blank intentionally

Decomposition of SoRo Rod Dynamics

- $\mathcal{M}_i^{\text{core}}$: composite mass distribution as a result of microsolid i's barycenter motion;
- $\mathcal{M}^{\text{pert}}$: motions relative to $\mathcal{M}_i^{\text{core}}$, considered as a perturbation;
- $\mathcal{M} = \mathcal{M}^{\text{pert}} \cup \mathcal{M}^{\text{core}}$.
- Introduce the transformation: $[\boldsymbol{q}, \dot{\boldsymbol{q}}] = [\boldsymbol{q}, \boldsymbol{z}]$, rewrite (2):

$$\boldsymbol{M}(\boldsymbol{q})\dot{\boldsymbol{z}} + [\boldsymbol{C}_1(\boldsymbol{q}, \boldsymbol{z}) + \boldsymbol{C}_2(\boldsymbol{q}, \boldsymbol{z}) + \boldsymbol{D}(\boldsymbol{q}, \boldsymbol{z})]\, \boldsymbol{z} - \boldsymbol{F}(\boldsymbol{q}) - \boldsymbol{N}(\boldsymbol{q})\text{Ad}_{\boldsymbol{g}_r}^{-1}\mathcal{G} = \tau(\boldsymbol{q})$$

Dynamics separation

Suppose that $\boldsymbol{M}^p = \int_{L^p_{\text{min}}}^{L^p_{\text{max}}} \boldsymbol{J}^\top \boldsymbol{\mathcal{M}}^{pert} \boldsymbol{J} dX$, and $\boldsymbol{M}^c = \int_{L^c_{\text{min}}}^{L^c_{\text{max}}} \boldsymbol{J}^\top \mathcal{M}^{core} \boldsymbol{J} dX$, then,

$$\boldsymbol{M}(\boldsymbol{q}) = (\boldsymbol{M}^c + \boldsymbol{M}^p)(\boldsymbol{q}), \ \boldsymbol{N} = (\boldsymbol{N}^c + \boldsymbol{N}^p)(\boldsymbol{q}), \tag{15a}$$

$$\boldsymbol{F}(\boldsymbol{q}) = (\boldsymbol{F}^c + \boldsymbol{F}^p)(\boldsymbol{q}), \quad \boldsymbol{D}(\boldsymbol{q}) = (\boldsymbol{D}^c + \boldsymbol{D}^p)(\boldsymbol{q}) \tag{15b}$$

$$\boldsymbol{C}_1(\boldsymbol{q}, \dot{\boldsymbol{q}}) = (\boldsymbol{C}_1^c + \boldsymbol{C}_1^p)(\boldsymbol{q}, \dot{\boldsymbol{q}}), \tag{15c}$$

$$\boldsymbol{C}_2(\boldsymbol{q}, \dot{\boldsymbol{q}}) = (\boldsymbol{C}_2^c + \boldsymbol{C}_2^p)(\boldsymbol{q}, \dot{\boldsymbol{q}}). \tag{15d}$$

Dynamics Separation

Furthermore, let

$$\boldsymbol{M} = \underbrace{\begin{bmatrix} \boldsymbol{\mathcal{H}} & 0 \\ 0 & 0 \end{bmatrix}}_{\boldsymbol{M}^c(\boldsymbol{q})} + \underbrace{\begin{bmatrix} 0 & \boldsymbol{\mathcal{H}}_{\text{slow}}^{\text{fast}} \\ \boldsymbol{\mathcal{H}}_{\text{slow}}^{\text{fast}\,\top} & \boldsymbol{\mathcal{H}}_{\text{slow}} \end{bmatrix}}_{\boldsymbol{M}^p(\boldsymbol{q})}, \tag{16}$$

where $\boldsymbol{\mathcal{H}}_{\text{slow}}^{\text{fast}}$ denotes the decomposed mass of the perturbed sections of the robot relative to the core sections.

- Let robot's state, $\boldsymbol{x} = [\boldsymbol{q}^\top, \boldsymbol{z}^\top]^\top$ decompose as $\boldsymbol{q} = [\boldsymbol{q}_{\text{fast}}^\top, \boldsymbol{q}_{\text{slow}}^\top]^\top$ and $\boldsymbol{z} = [\boldsymbol{z}_{\text{fast}}^\top, \boldsymbol{z}_{\text{slow}}^\top]^\top$,
- Define $\bar{\boldsymbol{M}}^p = \boldsymbol{M}^p/\epsilon$, and let $\boldsymbol{u} = [\boldsymbol{u}_{\text{fast}}^\top, \boldsymbol{u}_{\text{slow}}^\top]^\top$ be the applied torque.

SoRo Dynamics Separation

$$(\boldsymbol{M}^c + \epsilon \bar{\boldsymbol{M}}^p)\dot{\boldsymbol{z}} = \boldsymbol{s} + \boldsymbol{u}, \tag{17}$$

where

$$\boldsymbol{s} = \begin{bmatrix} \boldsymbol{s}_{\text{fast}} \\ \boldsymbol{s}_{\text{slow}} \end{bmatrix} = \begin{bmatrix} \boldsymbol{F}^c + \boldsymbol{N}^c \text{Ad}_{\boldsymbol{g}_r}^{-1} \boldsymbol{\mathcal{G}} - [\boldsymbol{C}_1^c + \boldsymbol{C}_2^c + \boldsymbol{D}^c]\boldsymbol{z}_{\text{fast}} \\ \boldsymbol{F}^p + \boldsymbol{N}^p \text{Ad}_{\boldsymbol{g}_r}^{-1} \boldsymbol{\mathcal{G}} - [\boldsymbol{C}_1^p + \boldsymbol{C}_2^p + \boldsymbol{D}^p]\boldsymbol{z}_{\text{slow}} \end{bmatrix}. \tag{18}$$

- Since $\boldsymbol{\mathcal{H}}_{\text{fast}}$ is invertible, let

$$\bar{\boldsymbol{M}}^p = \begin{bmatrix} \bar{\boldsymbol{M}}_{11}^p & \bar{\boldsymbol{M}}_{12}^p \\ \bar{\boldsymbol{M}}_{21}^p & \bar{\boldsymbol{M}}_{22}^p \end{bmatrix} \text{ and } \boldsymbol{\Delta} = \begin{bmatrix} 0 & 0 \\ \bar{\boldsymbol{M}}_{21}^p \boldsymbol{\mathcal{H}}_{\text{fast}}^{-1} & 0 \end{bmatrix}. \tag{19}$$

SoRo Dynamics Separation

Premultiplying both sides by $\boldsymbol{I} - \epsilon \boldsymbol{Delta}$, it can be verified that

$$\begin{bmatrix} \boldsymbol{\mathcal{H}}_{\text{fast}} & \bar{\boldsymbol{M}}_{12}^{p} \\ 0 & \bar{\boldsymbol{M}}_{22}^{p} \end{bmatrix} \begin{bmatrix} \dot{\boldsymbol{z}}_{\text{fast}} \\ \epsilon \dot{\boldsymbol{z}}_{\text{slow}} \end{bmatrix} = \begin{bmatrix} \boldsymbol{s}_{\text{fast}} \\ \boldsymbol{s}_{\text{slow}} - \epsilon \bar{\boldsymbol{M}}_{21}^{p} \boldsymbol{\mathcal{H}}_{\text{fast}}^{-1} \boldsymbol{s}_{\text{fast}} \end{bmatrix} + \begin{bmatrix} \boldsymbol{u}_{\text{fast}} \\ \boldsymbol{u}_{\text{slow}} - \epsilon \bar{\boldsymbol{M}}_{21}^{p} \boldsymbol{\mathcal{H}}_{\text{fast}}^{-1} \boldsymbol{u}_{\text{fast}} \end{bmatrix} \tag{20}$$

which is in the standard singularly perturbed form (9).

SoRo Fast Subsystem Extraction

- On the fast time scale $T = t/\epsilon$, with $dT/dt = 1/\epsilon$.
  - Dynamics: $\dot{\boldsymbol{z}}_{\text{fast}} = \dfrac{d\boldsymbol{z}_{\text{fast}}}{dt} \equiv \dfrac{1}{\epsilon}\dfrac{d\boldsymbol{z}_{\text{fast}}}{dT} \triangleq \dfrac{1}{\epsilon}\boldsymbol{z}'_{\text{fast}}$; and
  - $\epsilon\dot{\boldsymbol{z}}_{\text{slow}} = \boldsymbol{z}'_{\text{slow}}$.

Fast subdynamics:

$$\boldsymbol{z}'_{\text{fast}} = \epsilon\mathcal{H}^{-1}_{\text{fast}}(\boldsymbol{s}_{\text{fast}} + \boldsymbol{u}_{\text{fast}}) - \mathcal{H}^{-1}_{\text{fast}}\mathcal{H}^{\text{fast}}_{\text{slow}}\boldsymbol{z}'_{\text{slow}}, \tag{21a}$$

$$\boldsymbol{z}'_{\text{slow}} = \mathcal{H}^{-1}_{\text{slow}}(\boldsymbol{s}_{\text{slow}} - \boldsymbol{u}_{\text{slow}}) - \mathcal{H}^{-1}_{\text{fast}}(\boldsymbol{s}_{\text{fast}} - \boldsymbol{u}_{\text{fast}}) \tag{21b}$$

where the slow variables are frozen on this fast time scale.

SoRo Slow Subsystem Extraction

- We let $\epsilon \to 0$ in (20), so that what is left, i.e.,

$$\dot{\boldsymbol{z}}_{\text{slow}} = \mathcal{H}_{\text{slow}}^{-1}(\boldsymbol{s}_{\text{slow}} + \boldsymbol{u}_{\text{slow}}) \tag{22}$$

constitutes the system's slow dynamics; where the fast components are frozen on this slow time scale.

This page is left blank intentionally

Control of the Fast Strain Subdynamics

- Consider the transformation: $\begin{bmatrix} \boldsymbol{\theta} \\ \boldsymbol{\phi} \end{bmatrix} = \begin{bmatrix} \boldsymbol{q}_{\text{fast}} \\ \boldsymbol{z}_{\text{fast}} \end{bmatrix}$ so that $\boldsymbol{\theta}' = \epsilon \boldsymbol{z}_{\text{fast}} \triangleq \boldsymbol{\nu} :=$ A virtual input.
- Let $\{\boldsymbol{q}^d_{\text{fast}}, \dot{\boldsymbol{q}}^d_{\text{fast}}\} = \{\xi^d_1, \ldots, \xi^d_{n_\xi}, \boldsymbol{\eta}^d_1, \ldots, \boldsymbol{\eta}^d_{n_\xi}\}_{\text{fast}}$ be the desired joint space configuration for the fast subsystem.

Theorem 3 (Molu (2024))

The control law

$$\boldsymbol{u}_{fpos} = \boldsymbol{q}^d_{fast}(t_f) - \boldsymbol{q}_{fast}(t_f) + \boldsymbol{q}'^d_{fast}(t_f)$$

is sufficient to guarantee an exponential stability of the origin of $\boldsymbol{\theta}' = \boldsymbol{\nu}$ such that for all $t_f \geq 0$, $\boldsymbol{q}_{fast}(t_f) \in S$ for a compact set $S \subset \mathbb{R}^{6N}$. That is, $\boldsymbol{q}_{fast}(t_f)$ remains bounded as $t_f \to \infty$.

Control of the Fast Strain Subdynamics

Proof Sketch 1 (Proof of Theorem 3)

$$\boldsymbol{e}_1 = \boldsymbol{\theta} - \boldsymbol{q}^d_{fast}, \implies \boldsymbol{e}_1' = \boldsymbol{\theta}' - \boldsymbol{q}'^d_{fast} \triangleq \boldsymbol{\nu} - \boldsymbol{q}'^d_{fast}. \tag{23}$$

$$\textit{Choose } \boldsymbol{V}_1(\boldsymbol{e}_1) = \frac{1}{2}\boldsymbol{e}_1^\top \boldsymbol{K}_p \boldsymbol{e}_1 \tag{24}$$

$$\textit{Then, } \boldsymbol{V}_1' = \boldsymbol{e}_1^\top \boldsymbol{K}_p \boldsymbol{e}_1' = \boldsymbol{e}_1^\top \boldsymbol{K}_p(\boldsymbol{\nu} - \boldsymbol{q}'^d_{fast}). \tag{25}$$

For $\boldsymbol{\nu} = \boldsymbol{q}'^d_{fast} - \boldsymbol{e}_1$, $\boldsymbol{V}_1' = -\boldsymbol{e}_1 \boldsymbol{K}_p \boldsymbol{e}_1 \leq 2\boldsymbol{V}_1$.

Stability Analysis of the Fast Velocity Subdynamics

Theorem 4 (Molu (2024))

Under the tracking error $\boldsymbol{e}_2 = \boldsymbol{\phi} - \boldsymbol{\nu}$ *and matrices* $(\boldsymbol{K}_p, \boldsymbol{K}_q) = (\boldsymbol{K}_p^\top, \boldsymbol{K}_q^\top) > 0$, *the control input*

$$\boldsymbol{u}_{fvel} = \frac{1}{\epsilon}\mathcal{H}_{fast}[\boldsymbol{q}_{fast}^{\prime\prime d} + \boldsymbol{e}_1 - 2\boldsymbol{e}_2 - \boldsymbol{K}_q^\top(\boldsymbol{K}_q\boldsymbol{K}_q^\top)^{-1}\boldsymbol{K}_p\boldsymbol{e}_1] + \frac{1}{\epsilon}\mathcal{H}_{slow}^{fast}\boldsymbol{z}_{slow}^{\prime} - \boldsymbol{s}_{fast} \tag{26}$$

exponentially stabilizes the fast subdynamics (21).

Stability Analysis of Fast Velocity Subdynamics

Proof Sketch 2 (Sketch Proof of Theorem 4)

Recall from the position dynamics controller:

$$\begin{aligned} \boldsymbol{e}_1' &= \boldsymbol{\theta}' - \boldsymbol{q}_{fast}'^{d} \triangleq \boldsymbol{z}_{fast} - \boldsymbol{q}_{fast}'^{d} + (\boldsymbol{\nu} - \boldsymbol{\nu}) && (27a) \\ &= (\boldsymbol{\phi} - \boldsymbol{\nu}) + (\boldsymbol{\nu} - \boldsymbol{q}_{fast}'^{d}) \triangleq \boldsymbol{e}_2 - \boldsymbol{e}_1. && (27b) \end{aligned}$$

It follows that

$$\begin{aligned} \boldsymbol{e}_2' &= \boldsymbol{\phi}' - \boldsymbol{\nu}' = \boldsymbol{z}_{fast}' + \boldsymbol{e}_1' - \boldsymbol{q}_{fast}''^{d} && (28) \\ &= \mathcal{H}_{fast}^{-1}\left[\epsilon \boldsymbol{u}_{fast} + \epsilon \boldsymbol{s}_{fast} - \mathcal{H}_{slow}^{fast} \boldsymbol{z}_{slow}'\right] + (\boldsymbol{e}_2 - \boldsymbol{e}_1) - \boldsymbol{q}_{fast}''^{d}. \end{aligned}$$

Stability Analysis of the Fast Velocity Subdynamics

Proof Sketch 3 (Sketch Proof of Theorem 4)

For diagonal matrices $\boldsymbol{K}_p, \boldsymbol{K}_q$ with positive damping, let us choose the Lyapunov candidate function

$$\boldsymbol{V}_2(\boldsymbol{e}_1, \boldsymbol{e}_2) = \boldsymbol{V}_1 + \frac{1}{2}\boldsymbol{e}_2^\top \boldsymbol{K}_q \boldsymbol{e}_2 = \frac{1}{2}[\boldsymbol{e}_1 \;\; \boldsymbol{e}_2] \begin{bmatrix} \boldsymbol{K}_p & 0 \\ 0 & \boldsymbol{K}_q \end{bmatrix} \begin{bmatrix} \boldsymbol{e}_1 \\ \boldsymbol{e}_2 \end{bmatrix}.$$

If $\tilde{\boldsymbol{q}}_{fast} = \boldsymbol{q}_{fast} - \boldsymbol{q}^d_{fast}$ and $\tilde{\boldsymbol{q}}'_{fast} = \boldsymbol{q}'_{fast} - \boldsymbol{q}'^d_{fast}$, then the controller

$$\boldsymbol{u}_{fvel} = \frac{1}{\epsilon}\mathcal{H}_{fast}[\boldsymbol{q}''^d_{fast} - \tilde{\boldsymbol{q}}_{fast} - 2\tilde{\boldsymbol{q}}'_{fast} - \boldsymbol{K}_q^\top(\boldsymbol{K}_q\boldsymbol{K}_q^\top)^{-1}\boldsymbol{K}_p\tilde{\boldsymbol{q}}_{fast}] + \frac{1}{\epsilon}\mathcal{H}^{fast}_{slow}\boldsymbol{z}'_{slow} - \boldsymbol{s}_{fast},$$

exponentially stabilizes the system;

Stability Analysis of the Fast Velocity Subdynamics

Proof Sketch 4 (Sketch Proof of Theorem 4)

since it can be verified that

$$\begin{aligned} \boldsymbol{V}_2' &= \boldsymbol{e}_1^\top \boldsymbol{K}_p(\boldsymbol{e}_2 - \boldsymbol{e}_1) \\ &\quad - \boldsymbol{e}_2^\top \boldsymbol{K}_q \left(\boldsymbol{e}_2 - \boldsymbol{K}_q^\top (\boldsymbol{K}_q \boldsymbol{K}_q^\top)^{-1} \boldsymbol{K}_p \boldsymbol{e}_1\right) && \text{(29a)} \\ &= -\boldsymbol{e}_1^\top \boldsymbol{K}_p \boldsymbol{e}_1 - \boldsymbol{e}_2^\top \boldsymbol{K}_q \boldsymbol{e}_2 && \text{(29b)} \\ &\triangleq -2\boldsymbol{V}_2 \leq 0. && \text{(29c)} \end{aligned}$$

Stability analysis of the slow subdynamics

Set $\boldsymbol{e}_3 = \boldsymbol{z}_{\text{slow}} - \boldsymbol{\nu}$ so that $\dot{\boldsymbol{e}}_3 = \dot{\boldsymbol{z}}_{\text{slow}} - \dot{\boldsymbol{\nu}}$. Then,

$$\dot{\boldsymbol{e}}_3 = \dot{\boldsymbol{z}}_{\text{slow}} - \ddot{\boldsymbol{q}}^d_{\text{fast}} + (\boldsymbol{e}_2 - \boldsymbol{e}_1), \tag{30a}$$

$$= \mathcal{H}^{-1}_{\text{slow}}(\boldsymbol{s}_{\text{slow}} + \boldsymbol{u}_{\text{slow}}) - \ddot{\boldsymbol{q}}^d_{\text{fast}} + (\boldsymbol{e}_2 - \boldsymbol{e}_1). \tag{30b}$$

Theorem 5

The control law

$$\boldsymbol{u}_{slow} = \mathcal{H}_{slow}(\boldsymbol{e}_1 - \boldsymbol{e}_2 - \boldsymbol{e}_3 + \ddot{\boldsymbol{q}}^d_{fast}) - \boldsymbol{s}_{slow} \tag{31}$$

exponentially stabilizes the slow subdynamics.

Stability analysis of the slow subdynamics

Proof.

Consider the Lyapunov function candidate

$$\boldsymbol{V}_3(\boldsymbol{e}_3) = \frac{1}{2}\boldsymbol{e}_3^\top \boldsymbol{K}_r \boldsymbol{e}_3 \text{ where } \boldsymbol{K}_r = \boldsymbol{K}_r^\top > 0. \tag{32}$$

It follows that

$$\dot{\boldsymbol{V}}_3(\boldsymbol{e}_3) = \boldsymbol{e}_3^\top \boldsymbol{K}_r \dot{\boldsymbol{e}}_3 \tag{33a}$$

$$= \boldsymbol{e}_3^\top \boldsymbol{K}_r \left[\mathcal{H}_{\text{slow}}^{-1}(\boldsymbol{s}_{\text{slow}} + \boldsymbol{u}_{\text{slow}}) - \ddot{\boldsymbol{q}}_{\text{fast}}^d + \boldsymbol{e}_2 - \boldsymbol{e}_1\right]. \tag{33b}$$

Substituting $\boldsymbol{u}_{\text{slow}}$ in (31), it can be verified that

$$\dot{\boldsymbol{V}}_3(\boldsymbol{e}_3) = \boldsymbol{e}_3^\top \boldsymbol{K}_r \boldsymbol{e}_3 \triangleq -2\boldsymbol{V}_3(\boldsymbol{e}_3) \le 0. \tag{34}$$

Hence, the controller (31) stabilizes the slow subsystem. □

Stability of the singularly perturbed interconnected system

Let $\varepsilon = (0, 1)$ and consider the composite Lyapunov function candidate $\Sigma(\boldsymbol{z}_{\text{fast}}, \boldsymbol{z}_{\text{slow}})$ as a weighted combination of $\boldsymbol{V}_2$ and $\boldsymbol{V}_3$ i.e. ,

$$\boldsymbol{\Sigma}(\boldsymbol{z}_{\text{fast}}, \boldsymbol{z}_{\text{slow}}) = (1-\varepsilon)\boldsymbol{V}_2(\boldsymbol{z}_{\text{fast}}) + \varepsilon \boldsymbol{V}_3(\boldsymbol{z}_{\text{slow}}),\ 0 < \varepsilon < 1. \tag{35}$$

It follows that,

$$\begin{aligned}\dot{\boldsymbol{\Sigma}}(\boldsymbol{z}_{\text{fast}}, \boldsymbol{z}_{\text{slow}}) &= (1-\varepsilon)[\boldsymbol{e}_1^\top \boldsymbol{K}_p \dot{\boldsymbol{e}}_1 + \boldsymbol{e}_2^\top \boldsymbol{K}_q \dot{\boldsymbol{e}}_2] + \varepsilon \boldsymbol{e}_3^\top \boldsymbol{K}_r \dot{\boldsymbol{e}}_3, \\ &= -2(\boldsymbol{V}_2 + \boldsymbol{V}_3) + 2\varepsilon \boldsymbol{V}_2 \leq 0 \end{aligned} \tag{36}$$

which is clearly negative definite for any $\varepsilon \in (0, 1)$. Therefore, we conclude that the origin of the singularly perturbed system is asymptotically stable under the control laws.

$$\boldsymbol{u}(\boldsymbol{z}_{\text{fast}}, \boldsymbol{z}_{\text{slow}}) = (1-\varepsilon)\boldsymbol{u}_{\text{fast}} + \varepsilon \boldsymbol{u}_{\text{slow}}. \tag{37}$$

Asynchronous, time-separated control

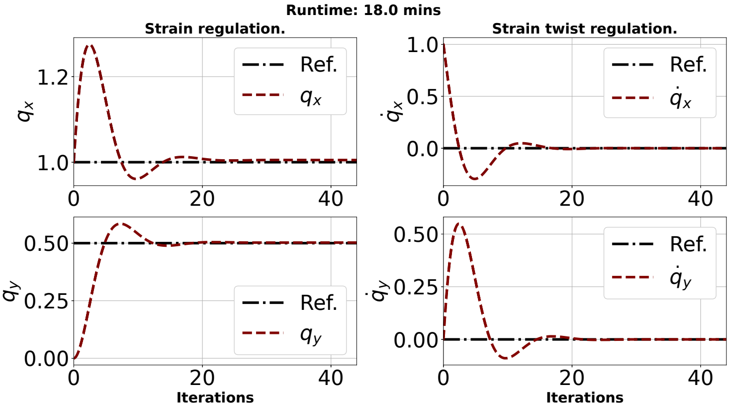

Ten discretized PCS sections: 6 fast, 4 slow subsections. $\mathcal{F}_p^y = 10\,N$, with $\boldsymbol{K}_p = 10$, $\boldsymbol{K}_d = 2.0$ for $\boldsymbol{\eta}^d = [0, 0, 0, 1, 0.5, 0]^\top$ and $\xi^d = 0_{6\times1}$.

Five-axes control

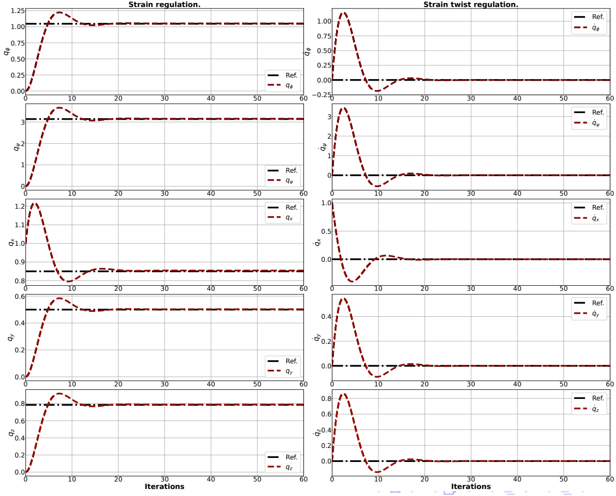

Time Response Comparison with Non-hierarchical Controller

Pieces			Runtime (mins)	
Total	Fast	Slow	Hierarchical SPT (mins)	Single-layer PD control (hours)
6	4	2	18.01	51.46
8	5	3	30.87	68.29
10	7	3	32.39	107.43

Table: Time to Reach Steady State.

References I

Cosimo Della Santina, Christian Duriez, and Daniela Rus. Model-based control of soft robots: A survey of the state of the art and open challenges. *IEEE Control Systems Magazine*, 43(3):30–65, 2023. doi: 10.1109/MCS.2023.3253419.

Derek E Moulton, Thomas Lessinnes, and Alain Goriely. Morphoelastic Rods III: Differential Growth and Curvature Generation in Elastic Filaments. *Journal of the Mechanics and Physics of Solids*, 142:104022, 2020.

Bartosz Kaczmarski, Alain Goriely, Ellen Kuhl, and Derek E Moulton. A Simulation Tool for Physics-informed Control of Biomimetic Soft Robotic Arms. *IEEE Robotics and Automation Letters*, 2023.

Mattia Gazzola, LH Dudte, AG McCormick, and Lakshminarayanan Mahadevan. Forward and inverse problems in the mechanics of soft filaments. *Royal Society open science*, 5(6):171628, 2018.

M. B. Rubin. *Cosserat Theories: Shells, Rods, and Points*. Springer-Science+Business Medis, B.V., 2000.

Eugène Maurice Pierre Cosserat and François Cosserat. *Théorie des corps déformables*. A. Hermann et fils, 1909.

Isuru S Godage, David T Branson, Emanuele Guglielmino, Gustavo A Medrano-Cerda, and Darwin G Caldwell. Shape function-based kinematics and dynamics for variable length continuum robotic arms. In *2011 IEEE International Conference on Robotics and Automation*, pages 452–457. IEEE, 2011.

Robert J. III Webster and Bryan A. Jones. Design and kinematic modeling of constant curvature continuum robots: A review. *The International Journal of Robotics Research*, 29(13):1661–1683, 2010.

Ke Qiu, Jingyu Zhang, Danying Sun, Rong Xiong, Haojian Lu, and Yue Wang. An efficient multi-solution solver for the inverse kinematics of 3-section constant-curvature robots. *arXiv preprint arXiv:2305.01458*, 2023.

Federico Renda, Vito Cacucciolo, Jorge Dias, and Lakmal Seneviratne. Discrete cosserat approach for soft robot dynamics: A new piece-wise constant strain model with torsion and shears. *IEEE International Conference on Intelligent Robots and Systems*, 2016-Novem:5495–5502, 2016. ISSN 21530866.

References II

Federico Renda, Frédéric Boyer, Jorge Dias, and Lakmal Seneviratne. Discrete cosserat approach for multisection soft manipulator dynamics. *IEEE Transactions on Robotics*, 34(6):1518–1533, 2018.

José Guadalupe Romero, Romeo Ortega, and Ioannis Sarras. A globally exponentially stable tracking controller for mechanical systems using position feedback. *IEEE Transactions on Automatic Control*, 60(3):818–823, 2014.

Lekan Molu and Shaoru Chen. Lagrangian Properties and Control of Soft Robots Modeled with Discrete Cosserat Rods. In *IEEE International Conference on Decision and Control, Milan, Italy*. IEEE, 2024.

Nikolai Matni, Aaron D Ames, and John C Doyle. A quantitative framework for layered multirate control: Toward a theory of control architecture. *IEEE Control Systems Magazine*, 44(3):52–94, 2024.

Lekan Molu. Fast Whole-Body Strain Regulation in Continuum Robots. *(submitted to) American Control Conference*, 2024.